THE JOURNAL OF BIOLOGICAL CHEMISTRY VOL. 282, NO. 50, pp. 36240–36249, December 14, 2007

Runx2- and Histone Deacetylase 3-mediated Repression Is Relieved in Differentiating Human Osteoblast Cells to Allow High Bone Sialoprotein Expression*

Received for publication, July 16, 2007, and in revised form, October 12, 2007 Published, JBC Papers in Press, October 22, 2007, DOI 10.1074/jbc.M705833200

Virginie Lamour[‡], Cédric Detry[‡], Christelle Sanchez[§1], Yves Henrotin[§], Vincent Castronovo[‡], and Akeila Bellahcène[‡2]

From the [‡]Metastasis Research Laboratory, Center of Experimental Cancer Research and [§]Bone and Cartilage Metabolism Research Unit, University of Liège, 4000 Liège, Belgium

Bone sialoprotein (BSP) is a bone matrix glycoprotein whose expression coincides with terminal osteoblastic differentiation and the onset of mineralization. In this study we show that BSP expression is considerably increased in confluent Saos-2 human osteosarcoma cells and in differentiating normal human osteoblasts, concomitantly with the decrease of Runx2, a key transcription factor controlling bone formation. Therefore, we investigated the role of Runx2 in the regulation of BSP expression in Saos-2 cells. Using a mobility shift assay, we demonstrated that Runx2 binds to the BSP promoter only in preconfluent cells. Histone deacetylase 3 (HDAC3) has been recently shown to act as a Runx2 co-repressor. Chromatin immunoprecipitation assays demonstrated that both Runx2 and HDAC3 are detectable at the BSP promoter in preconfluent Saos-2 cells but not when they are confluent and overexpress BSP. Consistently, nuclear Runx2 protein level is down-regulated, whereas Saos-2 cells became increasingly confluent. Finally, the suppression of HDAC3, Runx2, or both by RNA interference induced the expression of BSP at both mRNA and protein levels in Saos-2 cells. Our data demonstrate that Runx2 and HDAC3 repress BSP gene expression and that this repression is suspended upon osteoblastic cell differentiation. Both the nuclear disappearance of Runx2 and the non-recruitment of HDAC3 represent new means to relieve Runx2-mediated suppression of BSP expression, thus allowing the acquisition of a fully differentiated and mineralization-competent phenotype by osteoblast cells.

Bone sialoprotein (BSP)[3] is a glycoprotein that represents one of the major noncollagenous, extracellular matrix proteins associated with mineralized tissues (1, 2). High BSP expression coincides with *de novo* bone formation (3, 4). This bone matrix protein plays a major role during the formation and remodeling of bone, and it is considered as one of the primary markers of terminally differentiated osteoblasts (for review, see Ref. 5). BSP expression is induced by glucocorticoids (6–8), which promote osteogenic differentiation. On the contrary, it is inhibited by 1,25 dihydroxyvitamin D3, which suppresses the differentiation of osteoblasts and subsequent bone formation (9). We and others have shown that BSP is also expressed in osteotropic cancers and plays a role in the pathogenesis of bone metastasis (10–13). The study of the transcriptional regulation of the BSP gene is important not only to fully understand the mechanisms through which BSP is expressed in cells of osseous origin but also to potentially identify the basis of its ectopic expression in osteotropic cancer cells. Indeed, some transcriptional regulators of osteoblastic genes turned out to be also involved in the expression of these genes in breast and prostate cancer cells (14–16). More recently, we brought large-scale transcriptomic evidence of osteomimicry occurrence according to which the expression of bone-related genes may confer features of an osteoblast-like phenotype upon breast cancer cells (17).

Among several osteoblast-related transcription factors, Runx2 represents a key regulator in bone cells. It is a member of the runt/Cbfa family of transcription factors that is essential for the generation and maturation of osteoblasts and is a regulator of bone-specific gene expression (18, 19). Other Runx transcription factors include Runx1 and Runx3, which also have roles in skeletal development (20–22), although their regulatory functions are essentially exerted during hematopoiesis (23) and neural and gastrointestinal cell differentiation (24), respectively. Runx2 has been shown to regulate the expression of genes that characterize the osteoblast phenotype, including osteocalcin (OC), osteopontin, type I collagen, BSP, and collagenase 3 (18, 25–28). Because it is well established that BSP is a marker of osteoblastic differentiation and considering that Runx2 null mice do not express BSP (19, 29), one would expect Runx2 to be a positive regulator of BSP expression. However, Javed *et al.* (30), in their study of the *gallus* BSP gene promoter, demonstrated that Runx2 acts rather as a strong inhibitor of BSP expression in osseous and non-osseous cells. Far from the concept that Runx2 is a positive transcriptional regulator necessary to osseous gene expression, it now appears from several studies that Runx2 acts as a dual positive/negative regulator of gene expression depending on which cofactor is recruited. For

* This work was supported by grants from the National Fund for Scientific Research (NFSR) (Belgium), the Inter-University Attraction Pole (IAP-P5/31), and the University of Liège (Fonds Spéciaux), Belgium. We acknowledge the support of the European Commission through METABRE Contract CEE LSHC-CT-2004-503049. The costs of publication of this article were defrayed in part by the payment of page charges. This article must therefore be hereby marked "*advertisement*" in accordance with 18 U.S.C. Section 1734 solely to indicate this fact.

[1] A postdoctoral researcher at NFSR.

[2] A Research Associate of the NFSR. To whom correspondence should be addressed: Metastasis Research Laboratory, University of Liège, Tour de Pathologie, Bât B23, Sart-Tilman, 4000 Liège, Belgium. Tel.: 3243662557; Fax: 3243662975; E-mail: a.bellahcene@ulg.ac.be.

[3] The abbreviations used are: BSP, bone sialoprotein; HDAC3, histone deacetylase 3; TSA, trichostatin A; ChIP, chromatin immunoprecipitation; PIPES, 1,4-piperazinediethanesulfonic acid; EMSA, electrophoretic mobility shift assay; siRNA, small interfering RNA; OC, osteocalcin; RT, reverse transcription.

example, when it is associated with histone deacetylase 3 (HDAC3) at the OC promoter, Runx2 is able to repress OC expression in rat osteoblast cell lines (31). RNA-mediated interference-mediated suppression of HDAC3 in MC3T3-E1 osteoblasts accelerates mineralization and expression of OC, osteopontin, and BSP (31). HDAC3, is a class I member of the HDAC family, which are enzymes recruited by transcription factors to specific DNA regulatory sequences (32–34). Active expression of osteoblastic genes in mature osteoblasts and confluent ROS 17/2.8 osteosarcoma cells has been previously shown to involve histone H3 and H4 acetylation (35). Accordingly, HDACs inhibitors such as trichostatin A (TSA) and valproic acid promote osteoblast maturation (36, 37).

These observations prompted us to investigate the mechanism(s) through which BSP gene expression is considerably induced at the onset of mineralization and whether Runx2 and HDAC3 might intervene in this regulation. To answer these questions we used a Saos-2 human osteosarcoma cell culture model because it has been previously shown that these cells are able to undergo osteogenic differentiation and express BSP when forming mineralized tissue nodules in response to prolonged confluent culture (38). Indeed, these cells have been largely used as an osteoblast-like model on the basis of their (i) alkaline phosphatase and osteonectin production (39, 40), (ii) vitamin D receptor expression (41) and, (iii) bone matrix deposition ability (38, 42). Another advantage of the Saos-2 model is the fact that neither Runx1 nor Runx3 was detected in Saos-2 cells (25, 29, 43), and as such, this cell line represents one of the best cell lines available to specifically study gene regulation by Runx2.

In this study, we first demonstrated that endogenous BSP expression is significantly increased at both mRNA and protein levels along with confluence in the Saos-2 osteoblastic maturation model but also in normal human osteoblasts cultured in a differentiation medium. Taking advantage of the important induction of BSP expression in confluent *versus* pre-confluent Saos-2 cells, we next used mobility shift assay and chromatin immunoprecipitation techniques to compare the status of Runx2 and HDAC3 binding at the BSP promoter under both states of confluence. We found that at least one of the two putative Runx2 binding sites present in human BSP proximal promoter effectively binds Runx2 in pre-confluent Saos-2 cells and, to a far lower extent, in confluent cells. Consistently, when active expression of BSP is turned on in postconfluent cells, Runx2 is not detectable anymore in the nucleus using both Western blot and immunofluorescence techniques.

In vivo, immunoprecipitated Runx2 and HDAC3 are not present at the BSP promoter when Saos-2 cells become postconfluent. Finally, the suppression of Runx2, HDAC3, or both by RNA interference in preconfluent Saos-2 cells induces an increase in BSP expression. Our data demonstrate for the first time that Runx2 and HDAC3 exert a suppressive activity on BSP gene expression in human osteoblast cells that must be suspended in a specific and timely manner during osteoblast maturation to allow high BSP expression.

EXPERIMENTAL PROCEDURES

Cell Culture—Human osteosarcoma Saos-2 cells were routinely grown at 37 °C in a 5% CO_2 humidified atmosphere in Dulbecco's modified Eagle's medium containing 10% fetal bovine serum. Cells were cultured to different confluences: preconfluent (~50% confluence), confluent (~100% confluence), and postconfluent (confluent + 10 days of culture) and (confluent + 20 days of culture) when mentioned. Normal human osteoblasts were isolated from trabecular bone specimens obtained from patients undergoing knee replacement surgery. Bones were cut into small fragments, washed with Dulbecco's modified Eagle's medium, and then submitted to enzymatic digestions as previously described (44). Briefly, small pieces of bone (2 mm^3) were sequentially incubated with 0.5 mg/ml hyaluronidase type IV S (Sigma Aldrich) for 20 min at 37 °C and 0.6 mg/ml clostridial collagenase IA (Sigma-Aldrich) for 30 and 240 min successively at 37 °C (2 g of bone in 20 ml of enzymatic solution). The digested bone pieces were plated in T75 flasks and cultured in Dulbecco's modified Eagle's medium supplemented with 15% fetal calf serum, 10 mM HEPES, 100 units/ml penicillin, and 100 μg/ml streptomycin until osteoblasts migrated out of bone explants. At this point the medium was replaced with fresh medium containing 10% fetal calf serum, 10 mM HEPES, 100 units/ml penicillin, and 100 μg/ml streptomycin. When confluent, cells were collected and seeded in T75 flasks. Twenty-four hours after plating, the osteogenic differentiation medium (Dulbecco's modified Eagle's medium containing 10% fetal bovine serum, 10 mM β-glycerophosphate, and 50 ng/ml ascorbic acid) was added, and that point was designated day 0. At the end of this differentiation period, cells showed an osteoblastic phenotype characterized by the production of osteocalcin and alkaline phosphatase.

Antibodies—The monoclonal antibody which recognizes human BSP (LF-Mb24) (45) was kindly provided by Dr. L. W. Fisher (NIDCR, National Institutes of Health, Bethesda, MD). Polyclonal anti-p27 and anti-acetylhistone H3 were purchased from BD Biosciences and from Upstate Biotechnology (Waltham, MA) respectively. The polyclonal anti-HDAC3 was from Cell Signaling Technology (Danvers, MA). Polyclonal anti-Runx2 used for the mobility shift assay, immunoprecipitation, and the Western blot was from Abcam (Cambridge, MA). Antibodies directed against β-actin and tubulin were obtained from Sigma, and rabbit IgG was from Serotech (Burlington, ON, Canada).

Western Blot Analysis—Proteins were separated on SDS-polyacrylamide gels and transferred to polyvinylidene-difluoride Western blotting membrane (Roche Diagnostics). Membranes were blocked with 5% nonfat dry milk and 0.1% Tween 20 solution for 1 h at room temperature and incubated with the indicated primary antibodies. After washing, blots were incubated with a peroxidase-conjugated secondary antibody (Dako, Glostrup, Denmark) for 30 min. Blots were washed again and incubated in an ECL detection reagent (Amersham Biosciences). Tubulin was used as a cytoplasmic marker and β-actin as a control for equivalent protein loading.

Chromatin Immunoprecipitation (ChIP)—Saos-2 cells grown to the indicated density were transfected with the indicated small

interfering RNAs (siRNAs) or treated with 500 nM of TSA for 3 h. Formaldehyde was then added to the cell medium to a final concentration of 1%, and the cells were incubated for 10 min at room temperature with gentle shaking; glycine was added to a final concentration of 0.125 M, and cells were shaken for another 5 min. After removal of the medium, cells were washed twice in 5 ml of ice-cold phosphate-buffered saline containing a mixture of protease inhibitors (Roche Diagnostics). Cells were spun for 4 min at 2000 rpm at 4 °C, and pellets were resuspended in a cell lysis buffer (5 mM PIPES, (pH 8), 85 mM KCl, 0.5% Nonidet P-40, and protease inhibitors) and incubated for 10 min on ice. The lysates were spun for 5 min at 4000 rpm at 4 °C. The pellets were resuspended in a nuclei lysis buffer (50 mM Tris (pH 8), 10 mM EDTA, 1% SDS, and protease inhibitors) and incubated for 10 min on ice. The lysates were sonicated, and cellular debris was removed by centrifugation for 15 min at 4000 rpm at 4 °C in a microcentrifuge. Supernatant fractions were diluted 5-fold in a ChIP dilution buffer (0.01% SDS, 1.1% Triton X-100, 1.2 mM EDTA, 16.7 mM Tris (pH 8.1), 167 mM NaCl, and protease inhibitors). Each sample corresponded approximately to 2×10^6 cells. To reduce nonspecific background, each chromatin solution was precleared with 80 μl of salmon sperm DNA-protein A-agarose for 2 h at 4 °C with agitation. After the addition of antibodies, samples were incubated overnight at 4 °C with rotation. Immunocomplexes were collected with 60 μl of salmon sperm DNA-protein A-agarose for 2 h at 4 °C with rotation. Washes were done sequentially with the following; 0.1% SDS, 1% Triton X-100, 2 mM EDTA, 20 mM Tris-HCl (pH 8.1), and 150 mM NaCl; the same buffer containing 500 mM NaCl; 500 mM LiCl, 1% Nonidet P-40, 1% sodium deoxycholate, 1 mM EDTA, and 10 mM Tris-HCl (pH 8.1); Tris-EDTA, pH 8.0 (twice). Immunocomplexes were collected by repeated elutions with 250 μl of 1% SDS in 0.1 M $NaHCO_3$. NaCl was added to the combined eluates to a final concentration of 0.3 M, and protein-DNA was reverse cross-linked at 65 °C ON. RNase A (final concentration of 1 mg/ml) was added at 37 °C for 30 min. EDTA, Tris-HCl (pH 6.5), and proteinase K were added at a final concentration of 10 mM, 40 mM, and 40 μg/ml respectively, and samples were incubated for 1 h at 45 °C. DNA was recovered by phenol-chloroform extraction and ethanol precipitation. Fractions of the purified ChIP DNA (20%) or input (2%) were used for PCR analysis. Primers for PCR amplification of the BSP proximal promoter region DNA were 5′-ACATATTCGGAGCCCAAACTATTCA and 5′-GAACGTGGATTCTCACCAGAAAAC. PCRs were carried out for 27 cycles or 35 cycles when mentioned (94 °C for 30 s, 55 °C for 30 s, and 72 °C for 30 s), and final products were resolved on 6% polyacrylamide gels and visualized under ultraviolet light.

Nuclear Protein Extracts—Nuclear protein extracts were prepared according to the Dignam method (46). Briefly, Saos-2 cells were washed twice with 5 ml of ice-cold phosphate-buffered saline and collected by centrifugation at 1000 rpm for 5 min. The pellet was resuspended in washing buffer (10 mM Hepes pH 7.9, 20 mM KCl, 2 mM $MgCl_2$, 0.1 mM EDTA, 1 mM dithiothreitol, and protease inhibitors) by gentle pipetting. The pellet was collected by centrifugation during 2 min and resuspended in an Nonidet P-40 lysis buffer containing 10 mM Hepes (pH 7.9), 10 mM KCl, 2 mM $MgCl_2$, 0.1 mM EDTA, 0.2% Nonidet P-40, 1 mM dithiothreitol, and protease inhibitors and incubated on ice for 30 s. The nuclei pellet was collected by centrifugation at 6000 rpm for 5 min and resuspended in washing buffer. The pellet was again collected by centrifugation at 1,000 rpm for 2 min, resuspended in an extraction buffer (20 mM Hepes (pH 7.9), 1.5 mM $MgCl_2$, 0.2 mM EDTA, 630 mM NaCl, 25% glycerol, 0.5 mM dithiothreitol and protease inhibitors), and rocked in the cold room for 45 min followed by centrifugation at 14,000 rpm for 30 min. Aliquots of the supernatant containing nuclear proteins were stored at −80 °C. Protein concentrations were determined using a protein assay reagent (Micro BCA protein assay kit, Pierce).

Electrophoretic Mobility Shift Assay (EMSA)—Double-stranded oligonucleotidic probes were end-labeled by filling with Klenow enzyme (Invitrogen). The labeled probes were purified using a quick spin G25 Sephadex column (Roche Diagnostics) according to the manufacturer's instructions. EMSA reaction mixtures were prepared using 100 fmol of probe, 50 mM KCl, 12 mM Hepes, 1 mM EDTA, 1 mM dithiothreitol, 12% glycerol, 2 μg of poly(dI-dC), poly(dI-dC), and 5 μg of nuclear protein. After 30 min of incubation at room temperature, aliquots were loaded onto 6% polyacrylamide gel. The gel was electrophoresed for 2 h at 180 V, dried, and exposed to film for autoradiography. Probes used for the gel shift analysis included human BSP Runx2 sites (in bold); R1 Runx2 probe, 5′-TCTGGTGAGA**ATCCACG**TTCTGACA; R2 Runx2 probe, 5′-TCAATTAAA**TTCCACA**ATGCAAACCT. The probe comprising the consensus Runx2 site of the osteocalcin promoter, 5′-GCTGCAGT**CACCAA**CCACAGCATCCTTTGG, was used as a positive control (14). For supershift experiments, nuclear extracts and probes were subsequently incubated with anti-Runx2 antibody for 20 min.

siRNA Transfection—Saos-2 cells were transfected with siRNAs at a concentration of 25 nM for 48 h using the previously described calcium phosphate precipitation method (45). siRNAs specific to HDAC2 (5′-GCC UCA UAG AAU CCG CAU C), HDAC3 (5′-AAU CAG AAC UCA CGC CAG UAU), and Runx2 (5′-CUC UGC ACC AAG UCC UUU U (47), were used to silence the corresponding target genes. GL3 luciferase siRNA was used as an unrelated control (5′-CUU ACG CUG AGU ACU UCG A). All siRNAs and negative control siRNA (EGT) were purchased from Eurogentec.

RNA Extraction and Quantitative Real-time Reverse Transcription (RT)-PCR Analysis—Total RNA was isolated from Saos-2 cells using RNeasy columns (Qiagen) according to the manufacturer's instructions. First strand cDNA was synthesized using 2 μg of total RNA in 20 μl of RT reaction mixture containing 0.2 μg of pd(N)6 random hexamers (Amersham Biosciences), 2 mM each deoxynucleotide triphosphate (Eurogentec), 1× first strand buffer (50 mM Tris/HCl (pH 8.3), 75 mM KCl, 3 mM $MgCl_2$), 10 mM dithiothreitol, and 100 units of SuperScriptTM II RNase H RT (Invitrogen). The reverse transcriptase reaction was performed at 42 °C for 50 min before a 15-min inactivation step at 70 °C. Quantitative real-time PCR was performed in triplicate using the ABI Prism 7700 Sequence Detection System (Applied Biosystems, Foster City, CA) according to the manufacturer's instructions. BSP primers and a TaqMan probe were designed using the primer design

software Primer Express (Applied Biosystems) as previously described (45); BSP forward (5′-TGCCTTGAGCCTGCTTCCT), BSP reverse (5′-CTGAGCAAAATTAAAGCAGTCTTCA), BSP probe (6-carboxyfluorescein-5′-CCAGGACTGCCAGAGGAAGCAATCA-3′-6-carboxytetramethylrhodamine). The TaqMan glyceraldehyde-3-phosphate dehydrogenase (GAPDH) control reagent kit (Applied Biosystems) was used for GAPDH detection. cDNA samples (100 ng each) were mixed with 100 nM each of primer and TaqMan Universal PCR Master Mix containing 1× PCR buffer, 5.5 mM $MgCl_2$, 0.8 mM dNTPs mix, 100 nM probe, and 1 unit of AmpliTaq Gold® thermostable DNA polymerase (Applied Biosystems) in a total volume of 25 μl. Real-time PCR was conducted using the following parameters; 94 °C for 10 min, 45 cycles at 94 °C for 45 s, 57 °C for 45 s, and 72 °C for 45 s, and 72 °C for 2 min after the last cycle. Quantitative real-time PCR was performed for BSP and normalized to the amount of glyceraldehyde-3-phosphate dehydrogenase mRNA from the same sample. The acquired data were analyzed by Sequence Detector software, Version 1.9 (Applied Biosystems).

RESULTS

BSP Expression Is Increased with Saos-2 Cell Confluence—The Saos-2 human cell line represents an interesting model for studying mechanisms that control osteoblast-specific gene expression. It has been previously suggested that the confluence status of Saos-2 cells may influence the expression of bone-related genes such as BSP (38). Saos-2 cells were grown during increasing lengths of time corresponding to different confluence states: preconfluent (50%), confluent (100%), and postconfluent (confluent + 10 days and confluent + 20 days of culture). For each condition we quantified BSP expression at mRNA and protein levels using real-time RT-PCR and Western blotting techniques, respectively. BSP transcript expression was significantly increased in a confluence-dependent manner (Fig. 1*A*) with confluent + 20 days cells reaching about a 70-fold induction of BSP mRNA when compared with preconfluent cells. The expression of BSP was then examined by Western blot analysis using a monoclonal antibody directed against human BSP. Consistent with the induction observed at the mRNA level, confluent cells showed a significant increase in the BSP protein level when compared with less confluent cells (Fig. 1*B*).

The cyclin-dependent kinase inhibitors are key regulators of cell cycle progression. p27 is member of the Cip/Kip family of cyclin-dependent kinase (cdk) inhibitors and regulates cell growth by inactivating cell cycle stage-specific cdk-cyclin complexes. In osteoblastic cells, it has been previously shown that p27 levels are maximal postproliferatively (48). To assess whether Saos-2 osteosarcoma cells switched from a proliferating to a differentiating state in culture, we investigated the expression of p27 in pre- and postconfluent cells. p27 expression effectively increased in postconfluent cells and coincided with BSP overexpression (Fig. 1*C*).

Runx2 Binds to One of the Runx2 Binding Elements of the Human Proximal BSP Promoter, and Runx2 Complex Is More Important in Preconfluent Saos-2 Cells than in Confluent Cells—Runx2 is known to be a key regulator of osteogenic differentiation (19, 49), and as such, it controls the expression of several osteo-

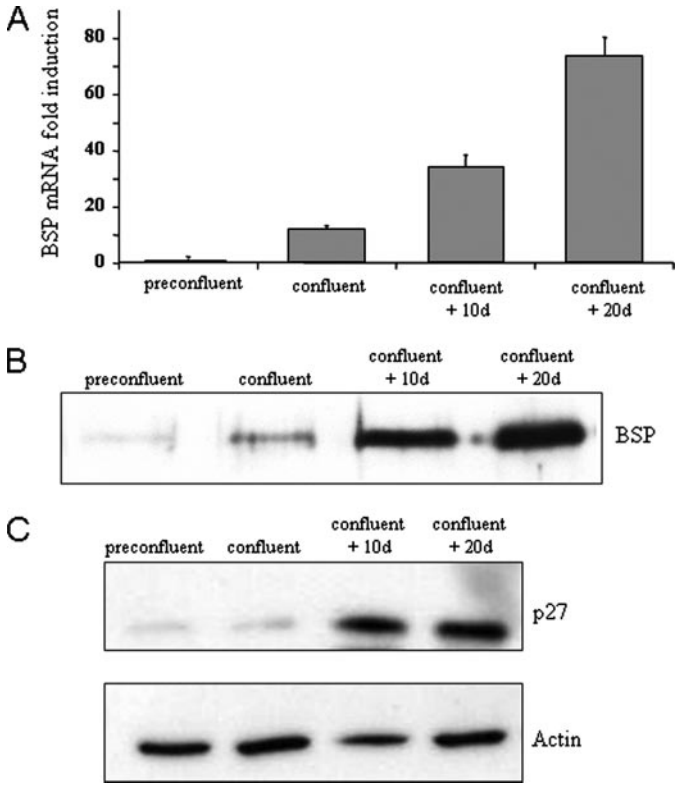

FIGURE 1. **BSP and p27 expression is increased with the confluence of Saos-2 human osteosarcoma cells.** *A*, Saos-2 cells were cultured to increasing confluence: preconfluent, confluent, confluent + 10 days, and confluent + 20 days (*d*) of culture. Total RNA extracts were analyzed by real-time quantitative RT-PCR, and histograms show the -fold induction of BSP mRNA as compared with the preconfluent condition arbitrarily set to 1. Mean values are expressed ±S.D. *B*, BSP protein expression was detected by Western blotting using a specific monoclonal antibody on total protein extracts from parallel cultures of Saos-2 cells as described above. *C*, Western blot for p27 on total proteins extracted from Saos-2 cells cultured to the same confluences as in *A*. Equal protein loading was assessed by anti-actin immunoblotting. Experiments were performed at least twice, and representative data from one experiment are shown.

blast-related genes (50). It has been recently shown that the BSP proximal promoter region in mice contains two Runx2 binding sites, and similar sequences have been located in human and rat promoters (51). However, the functional characterization of these putative Runx2 binding elements has never been reported for the human BSP proximal promoter. Although the inspection of the human BSP promoter sequence in the proximal region did not reveal perfect matches with the general Runt domain transcription factor consensus binding sequence (RCCRC(A/T)), two related sequences were identified at −83 bp (R1-ATCCACG) and −184 bp (R2-TTCCACA) (Fig. 2*A*). These sites are located within a highly conserved 343-bp region that shares 75% homology between mouse, rat, and human BSP gene promoters (52).

Double-stranded oligonucleotides containing the two putative Runx2 binding sites (R1 and R2) were labeled and used as probes in EMSA. A probe containing the consensus Runx2 binding site of the OC promoter was used as a positive control. Protein-DNA complexes co-migrating with the complex obtained using the consensus probe were observed for both R1 and R2 probes (Fig. 2*B*). These complexes were effi-

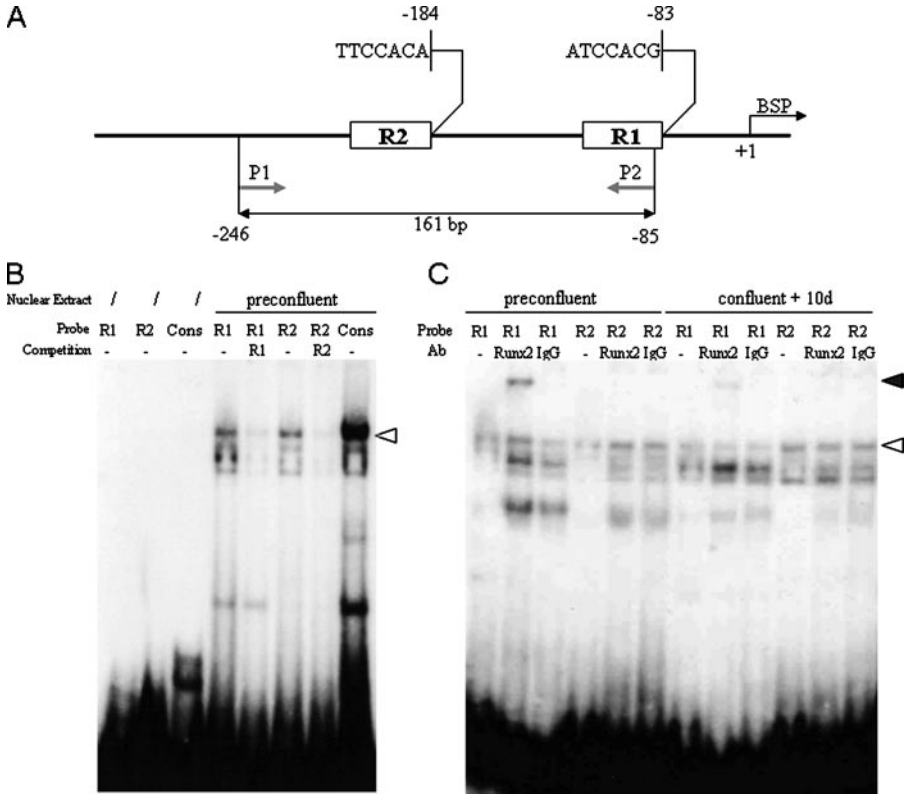

FIGURE 2. **Runx2 specifically interacts with the R1 Runx2 binding site of the BSP gene promoter in preconfluent Saos-2 cells.** *A*, schematic representation of Runx2 binding sites in the human BSP proximal promoter region. Putative Runx2 binding sites R1 and R2 are shown along with their position relative to the transcription start site. *P1* and *P2* indicate the localization of the PCR primers used in chromatin immunoprecipitation experiments. The position of these primers and the size of the expected fragment are indicated at the *bottom* of the *figure*. *B*, oligonucleotides containing R1 Runx2 binding (*probe R1*), R2 Runx2 binding site (*probe R2*) of the BSP promoter, and a probe containing the consensus Runx2 binding site of the osteocalcin promoter (*Cons*) used as a positive control were incubated with 5 μg of nuclear extracts from preconfluent Saos-2 cells. The *open arrowhead* represents the specific DNA-protein complex observed with all three probes. Competition assays performed with excess amounts of cold R1 and R2 probes demonstrate the specificity of the complex. *C*, preconfluent and confluent + 10 days Saos-2 cell nuclear extracts and probes were subsequently incubated with a specific anti-Runx2 polyclonal antibody or rabbit IgG. A supershifted complex was observed for the R1 probe, and not the R2, in the presence of anti-Runx2 antibody (*filled arrowhead*). Runx2 demonstrates a DNA binding activity at the R1 BSP promoter site when Saos-2 are preconfluent, which is no longer visible when the cells are in a postconfluent state. A representative experiment is shown ($n = 3$). *Ab*, antibody.

ciently competed using an excess of the corresponding cold probes, thus demonstrating the specificity of the binding (Fig. 2*B*). To assess the ability of the Runx2 transcription factor to bind to R1 and R2 sites *in vitro*, we performed supershift experiments using nuclear protein extracts from both preconfluent and confluent + 10 days Saos-2 cells and specific anti-Runx2 or rabbit IgG antibodies. The addition of the anti-Runx2 antibody led to the formation of a supershifted protein-DNA complex with the R1 but not R2 probe (Fig. 2*C*), whereas control IgGs had no effect on the migration of R1 and R2 complexes (Fig. 2*C*).

The Runx2 Nuclear Protein Level Is Decreased in Confluent Saos-2 Cells That Express High BSP Levels—EMSA analysis using specific anti-Runx2 antibodies demonstrated that the Runx2-supershifted complex was significantly increased in preconfluent Saos-2 cells when compared with confluent + 10 days cells (Fig. 2*C*). The nuclear Runx2 level is a critical determinant for its transcriptional activity during osteogenic differentiation. Therefore, we examined the level of Runx2 in cytoplasmic and nuclear protein extracts from pre- and postconfluent Saos-2 cells by Western blot. Nuclear Runx2 protein was dramatically lower in confluent + 10 days cell nuclear extracts than in preconfluent extracts (Fig. 3). The same blot probed with anti-tubulin demonstrates the purity of the nuclear fractions.

Increase of BSP Expression Coincides with Runx2 Decrease in Normal Human Osteoblast Cells—Next, we wanted to find out whether our observation of nuclear Runx2 decrease associated with BSP increase could be generalized to normal human osteoblast cells undergoing differentiation. We cultured normal osteoblasts in a defined differentiation medium containing 10 mM β-glycerophosphate and 50 ng/ml acid ascorbic and extracted total proteins and RNA from cells after 3, 7, and 14 days of culture. A Western blot analysis (Fig. 4*A*) using a specific anti-BSP antibody and real-time RT-PCR (Fig. 4*B*) demonstrated that at day 7 of osteoblastic differentiation BSP expression showed an increase at both protein and RNA levels that was concomitant to a significant decrease of Runx2 expression as revealed using a specific anti-Runx2 antibody (Fig. 4*A*).

Runx2 in Vivo Occupancy of Human BSP Proximal Promoters—We next used a ChIP technique to examine the presence of Runx2 at BSP proximal promoter region in both preconfluent and confluent + 10 days Saos-2 cells. Cross-linked and fragmented DNA-protein complexes were immunoprecipitated with either anti-Runx2, control IgG, or no antibody. PCR analysis on purified DNA was performed with primers that span Runx2 binding sites in the BSP promoter. The sequences and the positions of the primers selected for PCR analysis of ChIP DNAs are given under "Experimental Procedures" and in Fig. 2*A*, respectively. As shown in Fig. 5, BSP promoter DNA was amplified in samples from preconfluent cells but not from confluent + 10 days cells after immunoprecipitation with Runx2 antibody. These data indicate that Runx2 specifically interacts with the chromatin fragment containing Runx2 binding sites within the BSP promoter region and this only when the cells are in a preconfluent state. Input chromatin DNA-amplified products are shown as positive controls and attest for equivalent starting material. There was no significant amplification in samples col-

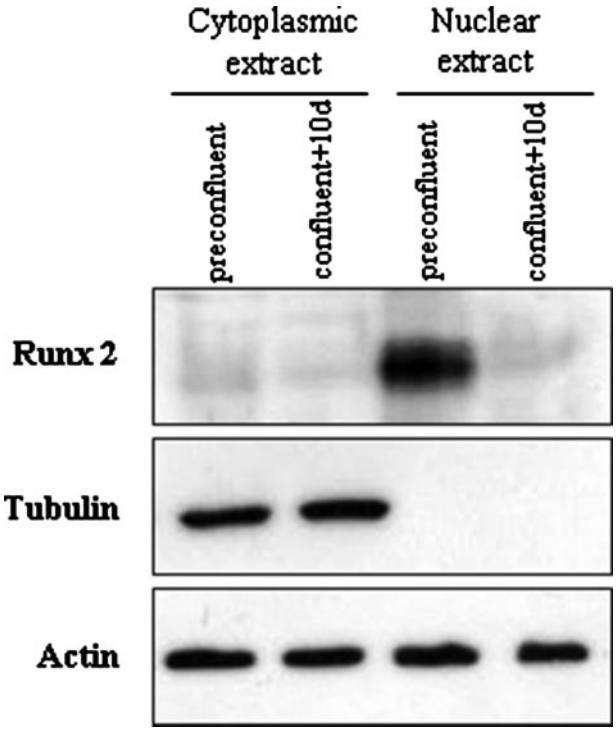

FIGURE 3. **Saos-2 cell confluence affects nuclear Runx2 expression.** Nuclear and cytoplasmic protein extracts were prepared from preconfluent and confluent + 10 days (*d*) Saos-2 cells and analyzed by Western blot. Cytoplasmic and nuclear fractions were also probed against a tubulin cytoplasmic marker, whereas actin was used as a loading control.

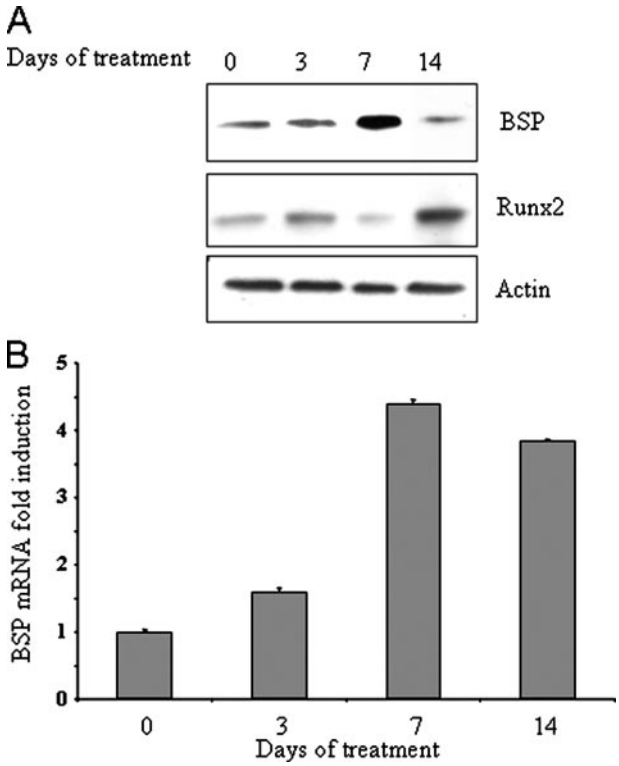

FIGURE 4. **Induction of BSP expression during normal human osteoblast differentiation is associated with a decrease of Runx2.** Normal osteoblasts were induced to differentiate by treatment with 10 mM β-glycerophosphate and 50 ng/ml ascorbic acid for 3, 7, and 14 days. *A*, whole cell lysates were prepared at these different time points and immunoblotted with anti-Runx2 and anti-BSP antibodies as described under "Experimental Procedures." Equal protein loading was assessed by anti-actin immunoblotting. *B*, total RNA extracts from parallel cultures of Saos-2 differentiating cells were analyzed by real-time quantitative RT-PCR. Histograms show the -fold induction of BSP mRNA as compared with day 0 condition arbitrarily set to 1. Mean values are expressed ±S.D. Each experiment was performed at least twice.

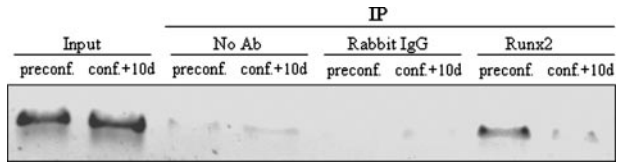

FIGURE 5. **Runx2 associates with the human BSP proximal promoter *in vivo*.** A ChIP assay was performed on preconfluent and confluent + 10 days *(conf. + 10d)* Saos-2 cells. Cells were cross-linked with formaldehyde, washed, lysed, and immunoprecipitated without any antibody (*No Ab*), rabbit IgG or Runx2 antibodies, as described under "Experimental Procedures." PCR performed using P1 and P2 primers (see Fig. 2*A*) shows significant amplification of the BSP proximal promoter in the input and Runx2 immunoprecipitate (*IP*) lanes. These results are representative of three independent experiments.

lected with beads alone (no antibody) or with anti-rabbit IgG antibody (Fig. 5).

Acetylated Histone H3 Proteins Are Detectable in the BSP Promoter in Saos-2 Cells Treated with Trichostatin A—The remodeling of chromatin is required to allow interactions of transcription factors and coregulators with their corresponding elements. The histone acetyltransferase inhibitor TSA has been reported to favor the overall acetylation status of histones, thus increasing the accessibility of specific chromatin regions to transcription factors (53). Acetylation level of histones H3 and H4 has been shown to be functionally coupled to the chromatin remodeling events that mediate OC gene transcription during osteogenesis (35). Therefore, we were interested to see whether TSA treatment has an influence on the histone acetylation status of the BSP proximal promoter in Saos-2 cells. To answer this question, ChIP experiments were performed on preconfluent Saos-2 cells treated with 500 nM TSA for 3 h. After cross-linking, chromatin was coprecipitated with an antibody to acetylated histone H3. PCR was performed using the same primers targeting the proximal BSP promoter as described above. The results of the ChIP showed that TSA induced the appearance of acetylated histone H3 at the BSP promoter compared with untreated cells (Fig. 6*A*). No amplification was observed in negative control samples of the ChIP procedure collected with no antibody and with anti-rabbit IgG antibody (Fig. 6*A*).

HDAC3 Associates with the Human BSP Promoter and Deacetylates Histone H3—HDAC3 has been shown to interact with Runx2 and to be associated with the rat OC promoter (31). Considering these data and our demonstration of the presence of Runx2 in the BSP promoter in Saos-2 cells, we next examined whether HDAC3 could also be recruited to the human BSP proximal promoter region. ChIP assays using a specific anti-HDAC3 antibody proved that HDAC3 is present at BSP promoter in Saos-2 cells (Fig. 6*B*), whereas it is not visible anymore after TSA treatment. Negative controls (no antibody and rabbit IgG) showed no amplification, and input chromatin amplification demonstrated equivalent starting material (Fig. 6*B*). This inverse association between the presence of HDAC3 and acetylated histone H3 proteins at the BSP promoter in Saos-2 cells upon treatment with TSA points to HDAC3 as a regulator of the acetylation status of the BSP promoter proximal region. To investigate whether the absence of acetylated histone H3 was

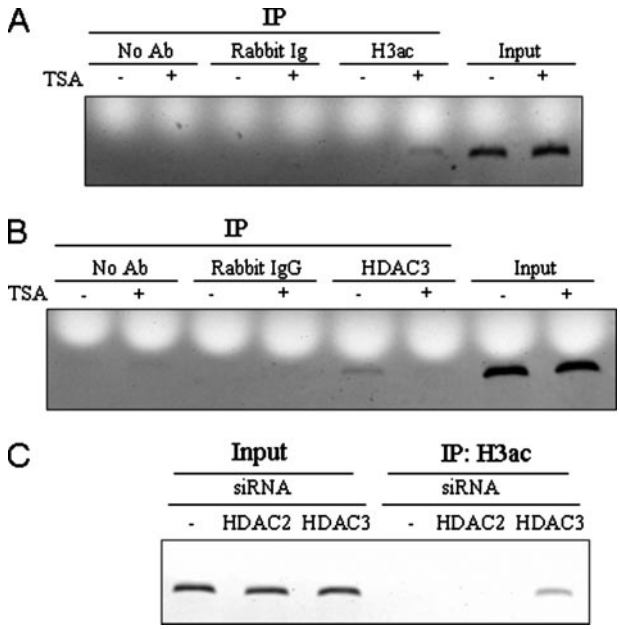

FIGURE 6. **The presence of acetylated histone H3 at the human BSP promoter is dependent upon the presence of HDAC3 and not HDAC2 class I HDACs.** Acetylated histone H3 (*H3ac*) (*A*) and HDAC3 (*B*) are associated with the BSP promoter in Saos-2 cells upon TSA treatment. Cross-linked chromatin prepared from Saos-2 cells treated with (+) or without (−) TSA was precipitated (*IP*) with the indicated antibodies, and PCR analysis was performed using primers specific for the BSP promoter region. *Ab*, antibody. *C*, enhanced histone H3 acetylation at the BSP promoter is observed upon HDAC3 silencing. Cross-linked chromatin prepared from Saos-2 cells transfected with the indicated siRNAs directed against HDAC2 and HDAC3 was immunoprecipitated with anti-acetylated histone H3 antibody, and PCR was performed using BSP primers as described under "Experimental Procedures." Representative results from one experiment are shown ($n = 3$).

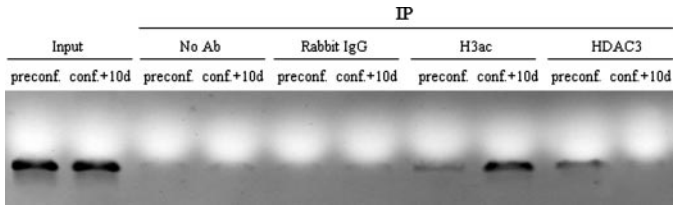

FIGURE 7. **HDAC3 is detectable at the BSP gene proximal promoter in preconfluent Saos-2 cells.** A ChIP assay was performed on preconfluent (*preconf*) and confluent + 10 days (*conf. + 10d*) Saos-2 cells with the use of 15 μg of the mentioned antibodies. HDAC3 association with the BSP promoter is more detectable in preconfluent than in confluent + 10 days Saos-2 cells. Accordingly, higher amounts of acetylated histone H3 (*H3ac*) were observed in confluent + 10 day cells when compared with preconfluent cells. PCR was performed using the same BSP proximal promoter primers as previously and was carried out for 35 cycles. Input amplification demonstrates equivalent starting material. Representative results from one experiment are shown ($n = 2$). *IP*, immunoprecipitate; *Ab*, antibody.

directly linked to the presence of HDAC3 at BSP promoter, we transfected Saos-2 preconfluent cells with an siRNA specifically directed against HDAC3. These cells were then processed for ChIP analysis using anti-acetylated histone H3 antibody in the immunoprecipitation step. We found that specific inhibition of HDAC3 expression significantly increased histone H3 protein acetylation at the BSP promoter (Fig. 6*C*). Indeed, the use of an siRNA directed against HDAC2, another class I HDAC, did not allow the appearance of histone H3 acetylated species at the BSP promoter (Fig. 6*C*).

Acetylated Histone H3, HDAC3, and Runx2 Are Detectable at the Proximal BSP Promoter in Saos-2 Cells in Vivo—Next, we addressed the question of whether the regulation of histone acetylation at the BSP promoter was affected in the same way in postconfluent Saos-2 cells that undergo osteogenic differentiation as under TSA treatment. For this purpose we performed ChIP experiments on preconfluent and confluent + 10 days Saos-2 cells. Cross-linked and fragmented DNA-proteins complexes were immunoprecipitated with either no antibody, anti-rabbit IgG, anti-acetylated histone H3, or anti-HDAC3 antibodies. As shown in Fig. 7, the amplification of BSP promoter DNA was detectable in samples collected with HDAC3 antibodies only when using preconfluent Saos-2 cell extracts. Acetylated histone H3 immunoprecipitates enabled the amplification of BSP promoter DNA more significantly under postconfluence than under preconfluence conditions. No amplification was detected in samples collected with beads alone (without antibody) and with anti-rabbit IgG antibody. PCR reactions with input DNA is shown as a control of the equivalent starting material. Overall, our ChIP experiments (Figs. 5 and 7) aimed at the comparison of the BSP promoter in terms of the presence of histone H3 protein acetylation, HDAC3, and Runx2, demonstrated that acetylated histone H3 proteins, an indicator of a transcriptionally permissive chromatin state, are detectable concomitantly with the disappearance of both HDAC3 and Runx2 from the BSP promoter in confluent + 10 days Saos-2 cells. Inversely, HDAC3 and Runx2 are associated with the BSP promoter in preconfluent cells only, a condition under which BSP expression is repressed.

HDAC3 and Runx2 Suppression Increases BSP Expression in Saos-2 Cells—Having demonstrated that Runx2 and HDAC3 do not associate with the BSP promoter in confluent Saos-2 cells that express high amounts of BSP, we next investigated the effect of HDAC3 and Runx2 suppression on endogenous BSP expression at protein and mRNA levels in Saos-2 preconfluent cells. Total RNA from HDAC3 and Runx2 siRNA-transfected cells was collected after 48 h of transfection and was used to perform a real-time RT-PCR. We observed that suppression of either HDAC3 or Runx2 or both induced a 10-, 3-, and 5-fold increase in BSP mRNA, respectively (Fig. 8*A*). The transfection of control siRNA directed against GL3 luciferase and a commercially available negative control siRNA (EGT) did not significantly affect BSP expression (Fig. 8*A*). A Western blot analysis performed on total proteins extracted from parallel siRNAs-transfected Saos-2 cells showed an increase in BSP protein when either the expression of HDAC3, Runx2, or both were specifically inhibited (Fig. 8*B*). These results indicate that both HDAC3 and Runx2 exert a suppressive activity on BSP gene expression in preconfluent Saos-2 cells. Runx2 and HDAC3 Western blots controlling the specific down-regulation of these proteins in siRNAs- transfected cells are presented in Fig. 8*B*.

DISCUSSION

BSP is a bone matrix glycoprotein that intervenes at different stages of bone remodeling. It acts as a nucleator of hydroxyapatite crystals via its glutamic acid-rich clusters (54). In addition, BSP is an RGD (Arg-Gly-Asp)-containing protein (2) that is able to interact with the osteoclast integrin $\alpha v\beta 3$ to potentiate

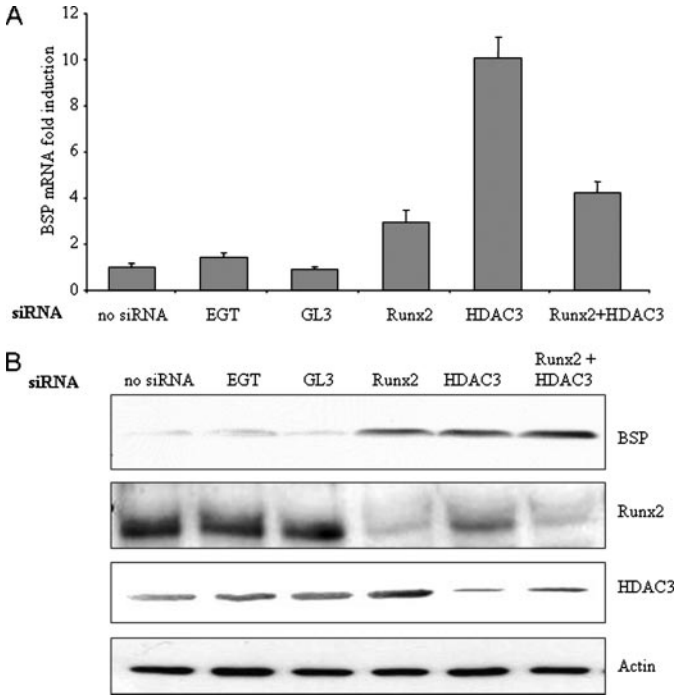

FIGURE 8. **HDAC3 and Runx2 suppression in Saos-2 cells increases BSP at mRNA and protein levels.** *A*, real-time quantitative RT-PCR was performed on the total RNA extracted from Saos-2 cells transfected with 25 nM concentrations of the indicated siRNAs for 48 h as described under "Experimental Procedures." Data are expressed as the mean ± S.D. *B*, Western blot analysis shows the increase of BSP protein levels in Saos-2 cells when Runx2, HDAC3, or both are silenced using specific siRNAs. Anti-Runx2 and anti-HDAC3 immunoblots confirmed the significant down-regulation of Runx2 and HDAC3 expression induced by the transfection of the corresponding siRNAs in Saos-2 cells. EGT and GL3 luciferase siRNAs represent a commercially available negative control and unrelated siRNA control, respectively. Equal protein loading was assessed by anti-actin immunoblotting. Representative results from one experiment are shown ($n = 2$).

bone resorption (55–57). The induction of BSP expression has been previously described as a strictly spatiotemporally regulated event during osteoblastic differentiation and subsequent extracellular matrix mineralization (8, 58). Runx2 is a critical regulator of bone formation and is required for osteoblast differentiation (18, 19) (59). It is a DNA-binding protein that can regulate both osteoblast-specific gene activation or repression. Although several studies have unveiled the mechanisms of Runx2-mediated transcriptional activation, much less is known about Runx2-mediated repression. The first demonstration of a negative transcription regulation by Runx2 for an osteoblast-expressed gene concerned the repression of the *gallus* BSP gene (30). In this study, the authors considered the possible intervention of known suppressors of Runx-dependent activation such as TLE/Groucho proteins (60, 61). However, neither coexpression of TLE1 or TLE2 nor the deletion of the TLE interaction motif of Runx2 relieved Runx2-mediated suppression of BSP expression (30).

In this study, we took advantage of the Saos-2 osteoblastic model (38) to investigate the mechanisms of human BSP gene transcriptional regulation by Runx2. Consistent with their osteoblastic cell behavior, we observed that Saos-2 cells maintained in culture for up to 20 days postconfluency entered a differentiation process that is accompanied by the expression of large amounts of BSP. The nonproliferative/differentiating status of the postconfluent Saos-2 cells was further confirmed by the demonstration of a high p27 expression level in comparison to preconfluent proliferating cells. p27 plays a key role in regulating osteoblast differentiation by repressing proliferation-related events in bone cells. Indeed, maximal p27 levels have been previously reported in postproliferative osteosarcoma cells (48).

We used EMSA and a Western blot analysis to assess both functional Runx2 binding to DNA and Runx2 nuclear content. We demonstrated that Runx2 is able to interact with the most proximal Runx2 binding sites of the BSP gene promoter when the cells are in a preconfluent status. This interaction does not occur anymore when Saos-2 cells reach postconfluency and overexpress BSP. We also observed that the transition of Saos-2 cells from a proliferative state to confluency is paralleled by the progressive disappearance of Runx2 from the nucleus. This observation is original since previous studies have generally reported that Runx2 mRNA and/or cellular protein levels remained constant or were increased during osteoblastic differentiation (62–64). It is likely that Runx2 is regulated at multiple levels (transcription, protein synthesis, subcellular localization, and DNA binding activity) during osteoblast differentiation *in vitro*. Our demonstration that nuclear levels of Runx2 vary during the osteoblastic differentiation process sheds light on an important point that must be considered in future Runx2 regulation studies.

Similar to the bone-specific OC gene, BSP is considered as a mature osteoblast gene that is up-regulated at the onset of bone matrix mineralization. Therefore, it is conceivable that both genes are expressed later than a series of other osteoblastic genes that need Runx2 activation. This hypothesis is further reinforced by the study of Liu *et al.* (65) which demonstrates that the overexpression of Runx2 in osteoblasts severely reduces OC expression. These data and ours strongly suggest that Runx2 acts as an inhibitor of osteoblastic maturation. Therefore, it is now more apparent that Runx2 presents dual functions depending on the maturational stage of the osteoblast; that is, a positive regulatory effect in the early stages of osteoblastic differentiation and a suppressive effect when osteoblasts adopt a more mature phenotype. Accordingly, Runx2 was recently described as an important player in maintaining a supply of immature osteoblasts (50).

Obviously, nuclear localization of a transcription factor is determinant for its control of target genes expression. Based on our observations, we suggest that Runx2 transcriptional activity can be rapidly controlled during osteoblastic differentiation by changes affecting its availability in the nucleus. Interestingly, neither a detailed analysis of Runx2 nuclear disappearance using confocal immunofluorescence microscopy (data not shown) nor Western blots on cytoplasmic fractions reveal the accumulation of Runx2 in the cytoplasm of postconfluent osteoblastic cells. This observation strongly suggests that when the expression of BSP is needed, Runx2 is rapidly exported and degraded in the cytoplasm or is degraded within the nucleus. The function of Runx2 in the osteogenic lineage is highly analogous to the role of the key transcription factor controlling the myoblast differentiation factor MyoD. The phosphorylation, ubiquitination, and rapid degradation in the cytoplasm of these

differentiation-associated transcription factors by cell cycle proteins have been previously reported (66–68). Nuclear degradation of proteins is being increasingly documented and appears to be another important mechanism for the rapid control of the activity of MyoD (69) and other crucial regulatory proteins such as p53 (70).

PEBP2β/Cbfβ is a Runx protein cotranscription factor that has been shown to protect Runx2 from ubiquitin-proteasome-mediated degradation (71). We considered the possibility that Runx2 disappearance from the nucleus in confluent Saos-2 cells was linked to a decrease in PEBP2β expression.

Western blots performed on nuclear and cytoplasmic fractions did not allow us to demonstrate any significant change in PEBP2β or subcellular localization in preconfluent *versus* postconfluent Saos-2 cells (data not shown). Additional experiments are obviously needed to reveal the exact mechanism leading to Runx2 disappearance from the nucleus in osteoblastic cells undergoing differentiation. Another interesting hypothesis to be explored is the role of inorganic phosphate signaling. Indeed, the requirement of inorganic phosphate (P_i) has been shown to be important during osteoblastic differentiation not only as a component of hydroxyapatite minerals but also as a signal event preceding mineralization (72). In their study of the role of P_i during mineralization, Fujita *et al.* (73) unexpectedly observed that P_i quickly evacuated Runx2 from the nuclei in osteoblastic MC3T3-E1 cells. Accelerated nodule formation and mineralization occurred the following days of culture, suggesting that this ultimate phase of osteoblastic differentiation does not necessitate the presence of nuclear Runx2, which concords with our data. In their study the expression of hydroxyapatite nucleator proteins such as BSP was not evaluated. However, the authors observed that P_i stimulus lowered the secretion of OC (73).

Nucleosomal histones are frequently hyperacetylated in transcriptionally active chromatin (32). We show that the BSP proximal promoter region contains low levels of acetylated histone H3 in preconfluent Saos-2 cells, whereas this level is significantly increased in confluent cells when BSP expression is highly induced. TSA-treated preconfluent cells also exhibited elevated levels of acetylated histone H3 at the BSP promoter. These results indicate that the BSP promoter shows a marked transition from a transcriptionally silent state to an active chromatin conformation after long-term culture and after TSA stimulation in Saos-2 cells. HDAC3 suppression in MC3T3-E1 cells undergoing differentiation induces the precocious expression of Runx2 target genes such as OC, osteopontin, and BSP (31). Our observation that TSA treatment significantly affected the level of HDAC3 at the BSP promoter is suggestive of a control of histone acetylation by this enzyme at the BSP proximal promoter. This was further confirmed by the presence of immunoprecipitable histone H3-acetylated species at the BSP promoter when HDAC3 expression is specifically blocked using siRNAs and not in the absence of another class I HDAC such as HDAC2. Furthermore, chromatin immunoprecipitation assays allowed us to show that the presence of HDAC3 at the BSP promoter exhibited the same pattern as Runx2, suggesting that this enzyme is probably recruited by Runx2, as recently shown for the OC promoter (31). When present in the nucleus, Runx2 could interact with HDAC3 to exert a repressive control on BSP transcription. In particular, we also demonstrated that the inhibition of either HDAC3 or Runx2 induces a significant increase in BSP expression. HDAC3 has been reported to be strictly nuclear and expressed throughout the osteoblastic differentiation process (31, 37), suggesting that this enzyme could be recruited to the BSP promoter by factors other than Runx2 to repress this latter activity. This is indeed possible since we observed the highest induction of endogenous BSP gene expression when HDAC3 is inhibited. Another possibility is that Runx2, in the absence of HDAC3, recruits other co-factors to behave as an inducer of BSP expression. However, the signals that switch Runx2 from a repressor to an activator remain to be identified. Overall, our data allow us to suggest that Runx2/HDAC3 interaction is a major and broad mechanism used by osteoblastic cells during differentiation for the tight control of multiple osteoblast-expressed genes.

This study shows the disappearance of endogenous Runx2 from the nucleus and the major decrease of its DNA binding activity at the BSP promoter in differentiating osteoblast cells, suggesting that Runx2 activity may interfere with the accomplishment of specific steps leading to osteoblast maturation and mineralization processes. Transcriptional activity of Runx2 must be very subtle and tightly regulated throughout the maturation process leading to fully differentiated osteoblasts. The Runx2 dual regulatory activity, repression and activation of osteogenic gene expression, suggested by our study is also illustrated by the fact that neither Runx2-deficient mice (19, 58) nor transgenic mice overexpressing Runx2 (65) present alterations in the bone formation process.

REFERENCES

1. Bianco, P., Fisher, L. W., Young, M. F., Termine, J. D., and Robey, P. G. (1991) *Calcif. Tissue Int.* **49,** 421–426
2. Fisher, L. W., McBride, O. W., Termine, J. D., and Young, M. F. (1990) *J. Biol. Chem.* **265,** 2347–2351
3. Chen, J., Shapiro, H., and Sodek, J. (1992) *J. Bone Miner. Res.* **7,** 987–997
4. Chen, J., Shapiro, S. S., Wrana, J. L., Reimers, S., Heersche, J. N. M., and Sodek, J. (1991) *Matrix* **11,** 133–143
5. Ganss, B., Kim, R. H., and Sodek, J. (1999) *Crit. Rev. Oral Biol. Med.* **10,** 79–98
6. Kasugai, S., Todescan, R., Jr., Nagata, T., Yao, K. L., Butler, W. T., and Sodek, J. (1991) *J. Cell. Physiol.* **147,** 111–120
7. Oldberg, A., Jirskog-Hed, B., Axelsson, S., and Heinegard, D. (1989) *J. Cell Biol.* **109,** 3183–3186
8. Yao, K. L., Todescan, R., Jr., and Sodek, J. (1994) *J. Bone Miner. Res.* **9,** 231–240
9. Kim, R. H., Li, J. J., Ogata, Y., Yamauchi, M., Freedman, L. P., and Sodek, J. (1996) *Biochem. J.* **318,** 219–226
10. Bellahcène, A., Merville, M. P., and Castronovo, V. (1994) *Cancer Res.* **54,** 2823–2826
11. Waltregny, D., Bellahcène, A., de Leval, X., Florkin, B., Weidle, U., and Castronovo, V. (2000) *J. Bone Miner. Res.* **15,** 834–843
12. Zhang, J. H., Tang, J., Wang, J., Ma, W., Zheng, W., Yoneda, T., and Chen, J. (2003) *Int. J. Oncol.* **23,** 1043–1048
13. Chen, J., Rodriguez, J. A., Barnett, B., Hashimoto, N., Tang, J., and Yoneda, T. (2003) *Connect Tissue Res.* **44,** Suppl. 1, 279–284
14. Barnes, G. L., Javed, A., Waller, S. M., Kamal, M. H., Hebert, K. E., Hassan, M. Q., Bellahcene, A., Van Wijnen, A. J., Young, M. F., Lian, J. B., Stein, G. S., and Gerstenfeld, L. C. (2003) *Cancer Res.* **63,** 2631–2637
15. Yang, J., Fizazi, K., Peleg, S., Sikes, C. R., Raymond, A. K., Jamal, N., Hu, M., Olive, M., Martinez, L. A., Wood, C. G., Logothetis, C. J., Karsenty, G., and Navone, N. M. (2001) *Cancer Res.* **61,** 5652–5659

16. Yeung, F., Law, W. K., Yeh, C. H., Westendorf, J. J., Zhang, Y., Wang, R., Kao, C., and Chung, L. W. (2002) *J. Biol. Chem.* **277,** 2468–2476
17. Bellahcène, A., Bachelier, R., Detry, C., Lidereau, R., Clezardin, P., and Castronovo, V. (2007) *Breast Cancer Res. Treat.* **1.1,** 135–148
18. Ducy, P., Zhang, R., Geoffroy, V., Ridall, A. L., and Karsenty, G. (1997) *Cell* **89,** 747–754
19. Komori, T., Yagi, H., Nomura, S., Yamaguchi, A., Sasaki, K., Deguchi, K., Shimizu, Y., Bronson, R. T., Gao, Y. H., Inada, M., Sato, M., Okamoto, R., Kitamura, Y., Yoshiki, S., and Kishimoto, T. (1997) *Cell* **89,** 755–764
20. Brenner, O., Levanon, D., Negreanu, V., Golubkov, O., Fainaru, O., Woolf, E., and Groner, Y. (2004) *Proc. Natl. Acad. Sci. U. S. A.* **101,** 16016–16021
21. Lian, J. B., Balint, E., Javed, A., Drissi, H., Vitti, R., Quinlan, E. J., Zhang, L., Van Wijnen, A. J., Stein, J. L., Speck, N., and Stein, G. S. (2003) *J. Cell. Physiol.* **196,** 301–311
22. Yoshida, C. A., Yamamoto, H., Fujita, T., Furuichi, T., Ito, K., Inoue, K., Yamana, K., Zanma, A., Takada, K., Ito, Y., and Komori, T. (2004) *Genes Dev.* **18,** 952–963
23. Okuda, T., van Deursen, J., Hiebert, S. W., Grosveld, G., and Downing, J. R. (1996) *Cell* **84,** 321–330
24. Li, Q. L., Ito, K., Sakakura, C., Fukamachi, H., Inoue, K., Chi, X. Z., Lee, K. Y., Nomura, S., Lee, C. W., Han, S. B., Kim, H. M., Kim, W. J., Yamamoto, H., Yamashita, N., Yano, T., Ikeda, T., Itohara, S., Inazawa, J., Abe, T., Hagiwara, A., Yamagishi, H., Ooe, A., Kaneda, A., Sugimura, T., Ushijima, T., Bae, S. C., and Ito, Y. (2002) *Cell* **109,** 113–124
25. Ducy, P., Starbuck, M., Priemel, M., Shen, J., Pinero, G., Geoffroy, V., Amling, M., and Karsenty, G. (1999) *Genes Dev.* **13,** 1025–1036
26. Jimenez, M. J., Balbin, M., Lopez, J. M., Alvarez, J., Komori, T., and Lopez-Otin, C. (1999) *Mol. Cell. Biol.* **19,** 4431–4442
27. Porte, D., Tuckermann, J., Becker, M., Baumann, B., Teurich, S., Higgins, T., Owen, M. J., Schorpp-Kistner, M., and Angel, P. (1999) *Oncogene* **18,** 667–678
28. Sato, M., Morii, E., Komori, T., Kawahata, H., Sugimoto, M., Terai, K., Shimizu, H., Yasui, T., Ogihara, H., Yasui, N., Ochi, T., Kitamura, Y., Ito, Y., and Nomura, S. (1998) *Oncogene* **17,** 1517–1525
29. Hoshi, K., Komori, T., and Ozawa, H. (1999) *Bone* (*NY*) **25,** 639–651
30. Javed, A., Barnes, G. L., Jasanya, B. O., Stein, J. L., Gerstenfeld, L., Lian, J. B., and Stein, G. S. (2001) *Mol. Cell. Biol.* **21,** 2891–2905
31. Schroeder, T. M., Kahler, R. A., Li, X., and Westendorf, J. J. (2004) *J. Biol. Chem.* **279,** 41998–42007
32. Lee, D. Y., Hayes, J. J., Pruss, D., and Wolffe, A. P. (1993) *Cell* **72,** 73–84
33. Hassig, C. A., and Schreiber, S. L. (1997) *Curr. Opin. Chem. Biol.* **1,** 300–308
34. Grunstein, M. (1997) *Nature* **389,** 349–352
35. Shen, J., Hovhannisyan, H., Lian, J. B., Montecino, M. A., Stein, G. S., Stein, J. L., and Van Wijnen, A. J. (2003) *Mol. Endocrinol.* **17,** 743–756
36. Schroeder, T. M., and Westendorf, J. J. (2005) *J. Bone Miner. Res.* **20,** 2254–2263
37. Lee, H. W., Suh, J. H., Kim, A. Y., Lee, Y. S., Park, S. Y., and Kim, J. B. (2006) *Mol. Endocrinol.* **20,** 2432–2443
38. McQuillan, D. J., Richardson, M. D., and Bateman, J. F. (1995) *Bone* (*NY*) **16,** 415–426
39. Murray, E., Provvedini, D., Curran, D., Catherwood, B., Sussman, H., and Manolagas, S. (1987) *J. Bone Miner. Res.* **2,** 231–238
40. Villarreal, X. C., Mann, K. G., and Long, G. L. (1989) *Biochemistry* **28,** 6483–6491
41. Ikeda, K., Imai, Y., Fukase, M., and Fujita, T. (1990) *Biochem. Biophys. Res. Commun.* **168,** 889–897
42. Rodan, S. B., Imai, Y., Thiede, M. A., Wesolowski, G., Thompson, D., Bar-Shavit, Z., Shull, S., Mann, K., and Rodan, G. A. (1987) *Cancer Res.* **47,** 4961–4966
43. Sudhakar, S., Katz, M. S., and Elango, N. (2001) *Biochem. Biophys. Res. Commun.* **286,** 74–79
44. Sanchez, C., Deberg, M. A., Piccardi, N., Msika, P., Reginster, J. Y., and Henrotin, Y. E. (2005) *Osteoarthritis Cartilage* **13,** 988–997
45. Chaplet, M., Detry, C., Deroanne, C., Fisher, L. W., Castronovo, V., and Bellahcene, A. (2004) *Biochem. J.* **384,** 591–598
46. Dignam, J. D., Lebovitz, R. M., and Roeder, R. G. (1983) *Nucleic Acids Res.* **11,** 1475–1489
47. Pratap, J., Javed, A., Languino, L. R., van Wijnen, A. J., Stein, J. L., Stein, G. S., and Lian, J. B. (2005) *Mol. Cell. Biol.* **25,** 8581–8591
48. Drissi, H., Hushka, D., Aslam, F., Nguyen, Q., Buffone, E., Koff, A., van Wijnen, A., Lian, J. B., Stein, J. L., and Stein, G. S. (1999) *Cancer Res.* **59,** 3705–3711
49. Banerjee, C., Javed, A., Choi, J. Y., Green, J., Rosen, V., van Wijnen, A. J., Stein, J. L., Lian, J. B., and Stein, G. S. (2001) *Endocrinology* **142,** 4026–4039
50. Komori, T. (2006) *J. Cell. Biochem.* **99,** 1233–1239
51. Roca, H., Phimphilai, M., Gopalakrishnan, R., Xiao, G., and Franceschi, R. T. (2005) *J. Biol. Chem.* **280,** 30845–30855
52. Benson, M. D., Aubin, J. E., Xiao, G., Thomas, P. E., and Franceschi, R. T. (1999) *J. Bone Miner. Res.* **14,** 396–405
53. Eberharter, A., and Becker, P. B. (2002) *EMBO Rep.* **3,** 224–229
54. Hunter, G. K., and Goldberg, H. A. (1994) *Biochem. J.* **302,** 175–179
55. Flores, M. E., Norgard, M., Heinegard, D., Reinholt, F. P., and Andersson, G. (1992) *Exp. Cell Res.* **201,** 526–530
56. Oldberg, A., Franzen, A., Heinegard, D., Pierschbacher, M., and Ruoslahti, E. (1988) *J. Biol. Chem.* **263,** 19433–19436
57. Ross, F. P., Chappel, J., Alvarez, J. I., Sander, D., Butler, W. T., Farach-Carson, M. C., Mintz, K. A., Robey, P. G., Teitelbaum, S. L., and Cheresh, D. A. (1993) *J. Biol. Chem.* **268,** 9901–9907
58. Ibaraki, K., Termine, J. D., Whitson, S. W., and Young, M. F. (1992) *J. Bone Miner. Res.* **7,** 743–754
59. Otto, F., Thornell, A. P., Crompton, T., Denzel, A., Gilmour, K. C., Rosewell, I. R., Stamp, G. W., Beddington, R. S., Mundlos, S., Olsen, B. R., Selby, P. B., and Owen, M. J. (1997) *Cell* **89,** 765–771
60. Javed, A., Guo, B., Hiebert, S., Choi, J. Y., Green, J., Zhao, S. C., Osborne, M. A., Stifani, S., Stein, J. L., Lian, J. B., van Wijnen, A. J., and Stein, G. S. (2000) *J. Cell Sci.* **113,** 2221–2231
61. Levanon, D., Goldstein, R. E., Bernstein, Y., Tang, H., Goldenberg, D., Stifani, S., Paroush, Z., and Groner, Y. (1998) *Proc. Natl. Acad. Sci. U. S. A.* **95,** 11590–11595
62. Banerjee, C., McCabe, L. R., Choi, J. Y., Hiebert, S. W., Stein, J. L., Stein, G. S., and Lian, J. B. (1997) *J. Cell. Biochem.* **66,** 1–8
63. Prince, M., Banerjee, C., Javed, A., Green, J., Lian, J. B., Stein, G. S., Bodine, P. V., and Komm, B. S. (2001) *J. Cell. Biochem.* **80,** 424–440
64. Shui, C., Spelsberg, T. C., Riggs, B. L., and Khosla, S. (2003) *J. Bone Miner. Res.* **18,** 213–221
65. Liu, W., Toyosawa, S., Furuichi, T., Kanatani, N., Yoshida, C., Liu, Y., Himeno, M., Narai, S., Yamaguchi, A., and Komori, T. (2001) *J. Cell Biol.* **155,** 157–166
66. Bae, S. C., and Lee, Y. H. (2006) *Gene* (*Amst.*) **366,** 58–66
67. Shen, R., Wang, X., Drissi, H., Liu, F., O'Keefe, R. J., and Chen, D. (2006) *J. Biol. Chem.* **281,** 16347–16353
68. Song, A., Wang, Q., Goebl, M. G., and Harrington, M. A. (1998) *Mol. Cell. Biol.* **18,** 4994–4999
69. Floyd, Z. E., Trausch-Azar, J. S., Reinstein, E., Ciechanover, A., and Schwartz, A. L. (2001) *J. Biol. Chem.* **276,** 22468–22475
70. Shirangi, T. R., Zaika, A., and Moll, U. M. (2002) *FASEB J.* **16,** 420–422
71. Huang, G., Shigesada, K., Ito, K., Wee, H. J., Yokomizo, T., and Ito, Y. (2001) *EMBO J.* **20,** 723–733
72. Beck, G. R., Jr. (2003) *J. Cell. Biochem.* **90,** 234–243
73. Fujita, T., Izumo, N., Fukuyama, R., Meguro, T., Nakamuta, H., Kohno, T., and Koida, M. (2001) *Biochem. Biophys. Res. Commun.* **280,** 348–352